Scanning Microscopy

Volume 1 | Number 3 Article 44

7-24-1987

Exposure of Vascular Smooth Muscle Cells for Analysis with the Scanning Electron Microscope

Bryan G. Miller
Indiana University School of Medicine

Andrew P. Evan
Indiana University School of Medicine

H. Glenn Bohlen
Indiana University School of Medicine

Scanning Microscopy, Vol. 1, No. 3, 1987 (Pages 1295-1313) 0891-7035/87$3.00+.00
Scanning Microscopy International, Chicago (AMF O'Hare), IL 60666 USA

EXPOSURE OF VASCULAR SMOOTH MUSCLE CELLS FOR ANALYSIS WITH THE SCANNING ELECTRON MICROSCOPE

Bryan G. Miller,* Andrew P. Evan, H. Glenn Bohlen

Department of Physiology & Biophysics and of Anatomy, Indiana University School of Medicine, 635 Barnhill Drive, Indianapolis, Indiana 46223

(Received for publication February 16, 1987, and in revised form July 24, 1987)

Abstract

There has been interest in using the scanning electron microsope (SEM) to study the structure of tissues obscured by other cellular or non-cellular elements almost since the SEM was first used to examine biological tissues. Such interest includes the vessel wall and, in particular, the vascular smooth muscle cells. This paper presents a review of the three basic methodologies that have been employed to allow examination of the vascular smooth muscle, 1) blunt dissection, 2) digestion and 3) microdissection. Discussion of other perivascular elements was not a focus of this review. Also presented is the application of these different methodologies to different pathophysiologic conditions.

Key Words: Arterioles, diabetes, morphometric analysis, vascular smooth muscle, Wistar Kyoto, Zucker, intestine

* Address for Correspondence:
Department of Zoology
Eastern Illinois University
Charleston, Illinois 61920
phone: 217-581-3126

Introduction

The realization that conditions such as hypertension, diabetes, or aging have distinct effects on the vasculature has accelerated the efforts to perform detailed qualitative and quantitative analysis of vascular smooth muscle (VSM) cell shape. Initially, these analyses could be performed only by assessing the shape of individual VSM cells reconstructed from serial sections(29,31,63) or one of several methods of morphometry.(1,3-9,20,24,32-36,43,46,47,50,56,64,67) The two major difficulties inherent in serial sectioning have been 1) the determination of the orientation of the sampled vessel in relation to the plane of section and 2) the amount of labor invested in the study of one or two cells. However, these reconstructions did provide the first estimate of VSM cell shape (Figure 1).

Morphometric methods using conventional LM or TEM sampling techniques have been used to study components of the vascular wall. The methodologies included point counting(32-35,46,64), planimeter measurements(47,50,67), thicknesses from wall areas(20,24,32,35,46,56), and calculating mean vessel dimensions derived from direct measurements.(1,3-9,30,36,43) Techniques of point counting were used to

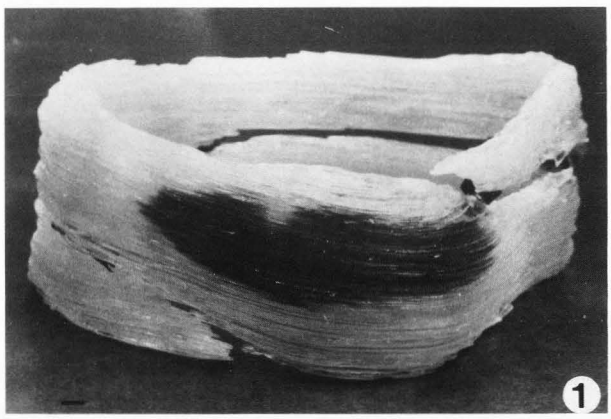

Figure 1. Reconstructed model of a terminal arteriole in hamster skeletal muscle. This VSM cell clearly was spindle-shaped and wrapped twice around the microvessel (17 μm lumen diameter). Bar = 1μm. from: Komuro et. al.,(31).

estimate the area of wall component(s) within a tissue or the portion of a tissue occupied by a given component (ie. area fraction). Planimeter measurements, which measure area more directly, are similar to methods of point counting because both techniques estimate area or area fractions of component(s). However, planimeter measurements may become meaningless if the vessel has been distorted or flattened. The average thickness of wall component(s) can be estimated directly from the inner and outer diameter associated with each wall component. However, vessel wall thickness depends in part upon the vessel diameter after fixation and preparation. Recent study has shown that vessel diameters may not be stable. Perfusion pressures <100 mmHg may stretch the vessel and create an increase in diameter at the expense of a thinner wall.(33) However, the cross-sectional area of arteriolar and arterial walls (40-700 μm lumen dia) has been shown to remain unchanged when the vessels were either relaxed (ie. vasodilated) or contracted.(16,33,68) Therefore, for an accurate comparison of wall characteristics between contracted and relaxed vessels, morphometric methods which calculate wall dimensions based on the cross-sectional wall areas should be used.(33) It has also been suggested that such methodology could be used to compare wall composition or dimensions between different strains of animals.(32-35,46,55)

Mulvany et. al.,(46) used vessel diameters calculated from wall area measurements and "a three-dimensional dissector" described below, after the method of Sterio(59), to estimate cellular dimensions from mesenteric resistance vessels of spontaneously hypertensive and Wistar-Kyoto rats. The authors did not perform routine serial sectioning, wherein sections are taken perpendicular to the long axis of the vessel; they took serial sections of the vessel wall that were parallel to the long axis of the vessel. This elegant method has simplified the determination of cell dimensions within a vessel wall and avoided the fundamental problem of sampling large 'particles' (e.g., portions of cells) more frequently than small 'particles' by using randomly selected volumes of the vessel wall. This methodology would not be applicable, as described, to smaller vessels whose circumference was close to the average length of the VSM cell. In such vessels, one would have to be concerned about sampling the same cell more than once because the cell encircled the vessel wall.

Much information has been gained from the techniques noted above, but none of the morphometric methodologies allow the actual analysis of an individual VSM cell. In addition, these methods have several inherent complications that must be carefully accounted for: 1) knowing the sampled vessel's orientation relative to the plane of section, 2) knowing the sampled vessel's precise location within the vascular system, and 3) obtaining a sample size large enough to provide meaningful data.(morphological(1,65) and anatomical(53,57) reviews)

The scanning electron microscope (SEM) is appropriate for examining vessel or cell structure in that one can obtain a three-dimensional image of a specific cell or vessel as well as being able to survey large numbers of the cells or vessels in question without having to prepare separate specimens. However, use of routine SEM procedures to evaluate vascular walls, other than the endothelium, is severely limited because all other surfaces are covered by connective tissue elements. In order to make use of SEM, a variety of approaches have been explored to circumvent this problem: 1) blunt dissection, 2) tissue digestion, and 3) a combination of dissection and digestion.

Blunt Dissection

Blunt dissection involves splitting open the sample of tissue either randomly or within a region of interest. This technique may occasionally remove portions of obscuring tissue without severely damaging the cells of interest. Cope and Roach(15) partially stripped away a portion of the intima from one human cerebral artery obtained from autopsy. In this fashion, the authors wished to expose the VSM and connective tissue fibers within the media. They found that the various components within the media were "difficult to differentiate" after simple fixation and stripping. Therefore, they added a silver nitrate stain in the hope that it may "be successful in outlining ... smooth muscle cells". They felt this added treatment made the VSM cells visible. VSM cells were described as having a roughly circumferential pitch, a diameter of 2-5 μm, and a length of 30-50 μm.

Boyde and Wood(10) suggested that dissecting and ripping of aldehyde-perfused and fixed tissue was a method for inducing "artificial surfaces". They noted that the duration of fixation influenced how the tissue might separate. The authors also suggested that enzymatic digestion may be useful, but it must precede fixation and that superior preservation of surface detail might be obtained by drying tissue by the critical point method. Performing the dissection after the tissue has been dried by the critical point method(2,14) can improve the results obtained by blunt dissection, because most specimens would tend to separate along anatomical planes of connective tissue or between different types of tissue. Miller and Revel(44) used simple dissection methods to visualize the three-dimensional shape of epithelial cell *in situ*, after drying by the critical point method. This study suggested that the high degree of complexity within an epithelia was produced by the interaction of lateral surfaces between intestinal, kidney, or embryonic epithelial cells. As may be apparent, blunt dissection, regardless of when employed, was severely limited by the lack of reproducibility and specificity. Another limitation was the presence of residual connective tissue elements or intercellular ground substance(s) that

remained attached to the surface of the cell(s) of interest.

Castenholz and others, using rat cerebral vascular systems that were either injected or not injected with a casting resin, exposed the periendothelial cells around cerebral arterioles and capillaries without digestion by exposing the brains to ultrasonic treatment.(11-13) The uncasted ultrasound treated cerebral vessels demonstrated a complete tunic of periendothelial smooth muscle.(12) The adventitial surface of the VSM cells were still covered by a fine network of fibrous matter, identified as the basement membrane material. The casted vessels were examined, but residual "adventitial tissue" prevented a clean exposure of VSM cells (Figure 2). Castenholz and others also used KOH digestion to completely remove all tissue from rat cerebral vascular systems injected with casting resin. These studies demonstrated "plastic strips", replicas of the periendothelial cells that constitute the muscle layer of cerebral arterioles and surround the capillaries.(11-13) These serendipitous replicas were found only in terminal arterial vessels (Figure 3). Their etiology was not known. Casting the vasculature could improve one's ability to locate where any exposed VSM cells are within the vascular system because the cast would survive the handling and processing associated with dissection. However, what cells were exposed or replicated as "plastic strips" was random and, therefore, not reproducible.

Although it seemed that blunt dissection techniques might produce good results, the problems of limited reproducibility and specificity could not be avoided. The exposure of specific cell(s) of interest was essentially a random phenomenon.

Digestion

Digestion techniques have been employed in an effort to circumvent the problems encountered with blunt dissection. Digestion methods specific to a particular tissue might allow reproducible exposure of vessels or embedded structures. Since collagen is the predominant extracellular material obscuring the surfaces of most cells, collagenase was one of the first corrosive materials used to expose cell surfaces for SEM analysis, with varying levels of success. Spencer and Lieberman(58) showed that the endoneural collagen in peripheral nerves was not completely removed by collagenase. Dyck and Lais(17) reported the introduction of artifacts ("broken membranes and watery spaces") when attempting collagenase digestion of a human sural nerve. Several studies showed only limited exposure of fine surface detail with other corrosive solutions, such as hyaluronidase, a-amylase, or sodium bromide.(19,52,60)

Evan et. al.,(18) developed a two-step digestion protocol that could selectively and reproducibly remove the basement membrane and collagen without destroying the integrity of the underlying cell surfaces (Figures 4a,c). Hydrochloric acid (HCl) and collagenase were applied to kidney, skin, and neural tissue. Critical steps in this method were: 1) fixing the tissue prior to digestion, 2) the sequence of digestion (HCl before collagenase II), 3) time of exposure to HCl, and 4) the type of collagenase. Previously scanned specimens also were removed from their supports and passed through the steps of infiltration and embedment in Epon 812 (Figure 4). Light microscopy (LM) sections (1 um thick) were stained with toluidine blue. Thin sections (<10 n thick) were stained with uranyl acetate and lead citrate and examined by transmission electron microscopy (TEM). Untreated specimens were sectioned for comparison (Figures 4b,d). Despite the exposure to HCl, the cytoarchitecture was adequately preserved (Figures 4e,f). The plasmalemma and mitochondrial

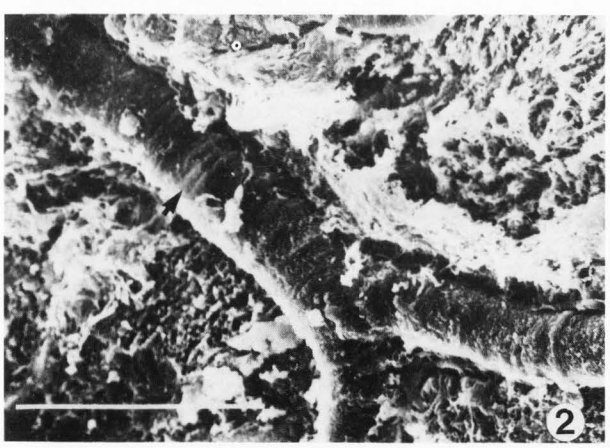

Figure 2. Cerebral arteriole from the rat. The rat was perfused with 2.5% glutaraldehyde via the heart and injected with resin via the common carotid artery. Material identified as "adventitial tissue of the vascular wall" still obscured examination of the ringlike prominences (arrow) that proved to be "plastic strips". Bar = 20µm. from: Castenholz et. al.,(13).

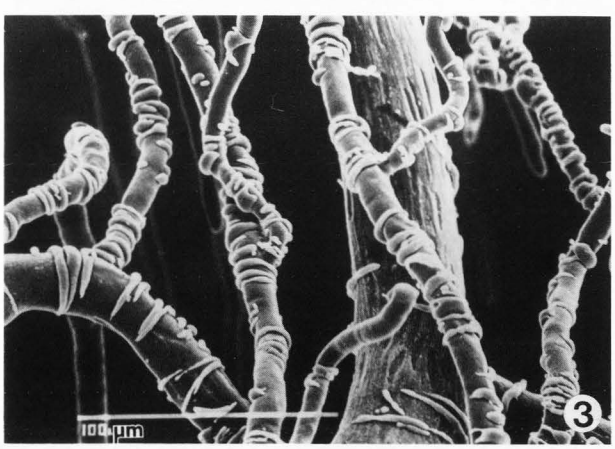

Figure 3. A cast of the rat cerebrum showing several arterioles with their branches. A small artery (running from top to bottom on the right side) was also evident. Note that the "plastic strips" were not continuous over the vessels. Bar = 100µm. from: Castenholz et. al.,(13).

membranes of kidney tubules retained their normal trilaminar appearance (Figure 4f). However, the nuclei suffered notable damage. The autonomic ganglia experienced slight distortion of the ganglion cell(s) and the surrounding satellite cells, but much of this was due to the removal of the collagen bundles that occupied the extracellular spaces.

Other investigators also used the basic HCl-collagenase method of Evan et. al.,(18) to expose vessels from other sources. Uehara and Suyama(62) tried two approaches. They used the method of Evan et. al., (18) to expose the smooth muscle layer of arterioles from the hamster cheek pouch (Figure 5). The authors also used a method of digesting the tissue with collagenase plus trypsin prior to fixation to expose central retinal vessels of the rat (Figure 6). The quality of exposure expressed in terms of selectivity and consistency produced by the two methods was judged to be equivalent. However, the

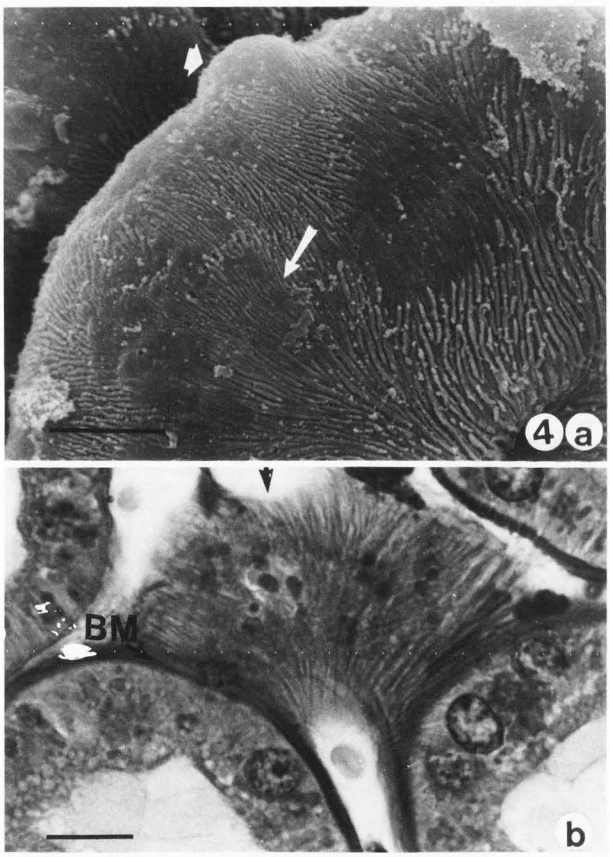

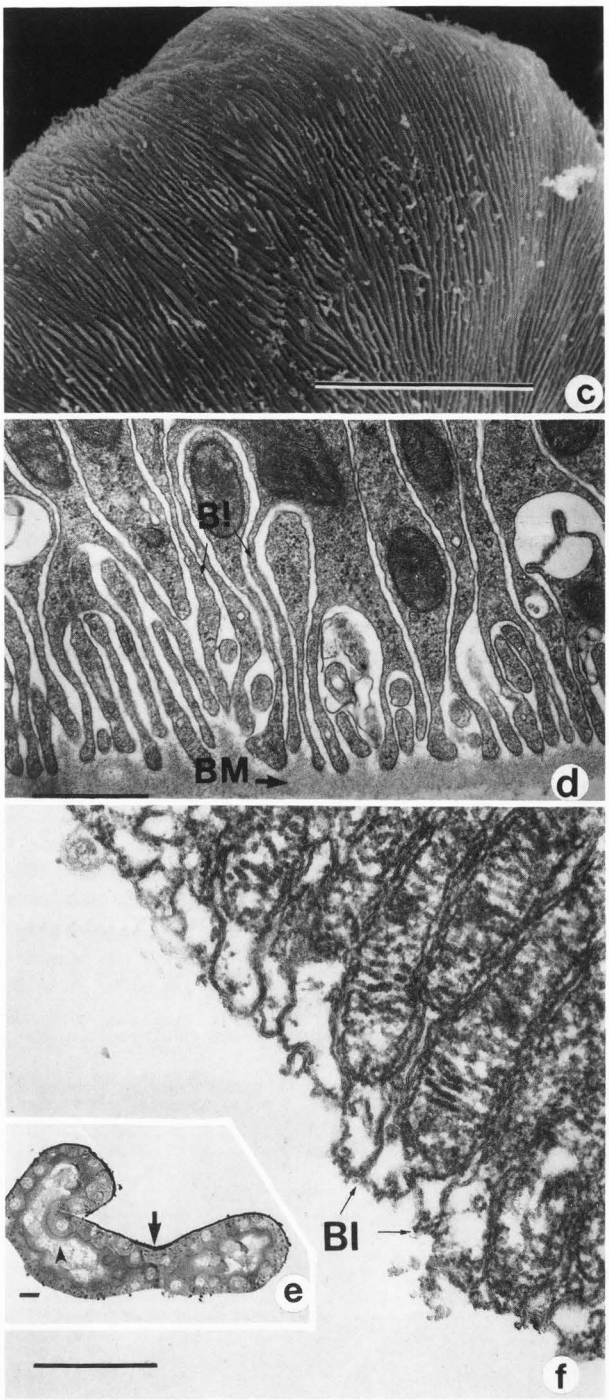

Figure 4. HCl and collagenase-treated proximal convoluted tubule in the rat. **a.** SEM showing elevations and areas devoid of prominent ridges (arrowhead) existing among the more extensive regions having basal ridges (arrow). Bar = 10μm. **b.** Light micrograph of a PAS- stained proximal convoluted tubule showing its striated basal surface (arrow). The striations were largely parallel and corresponded to the ridges seen in **a.** This section was not processed by the method of Evan et. al.,(18). Basement membrane (BM). **c.** SEM of a proximal convoluted tubule exposed by the method of Evan et. al.,(18). Removal of the basement membrane revealed parallel ridges corresponding to basilar interdigitations identified in **d.** Bar = 10μm. **d.** TEM micrograph of the basal surface of the proximal convoluted tubule. This section was not processed by the method of Evan et. al.,(18). Note the thick basement membrane (BM) and the basal interdigitations (BI). Bar = 1μm. **e.** A one micron section of the proximal tubule seen in **c.** Note the intact brush border (arrowhead) and the coat of Au-Pd alloy (arrow) from sputter coating for SEM. Bar = 10μm. **f.** TEM micrograph of the basal surface seen in **c.** and **e.** Note the lack of basement membrane. Basal interdigitations (BI). Bar = 1μm. from: Evan et. al.,(18).

authors expressed concern for the unavoidable introduction of some artifacts by the exposure to HCl. Possible artifacts produced by the collagenase/trypsin method were not discussed. Murakami et. al.,(48) reported that the collagenase/trypsin method did not consistently remove extracellular materials, and occasionally would disrupt the cell surface. The authors also reported the successful exposure of retinal capillaries by the HCl-collagenase method. Shimada(54) used the method of Evan et. al., (18) to expose the lymphatic and blood capillaries of the monkey thyroid gland. Injecting a casting resin into the vascular system accentuated the three-dimensional structure of the capillary network (Figure 7). Shimada noted that the method of Evan et. al.,(18) would effectively remove interstitial connective tissue elements and afford an opportunity to view directly the topographical relationships among various vessels and their perivascular components. However, he noted that the time and temperature for treatment with HCl should be determined by trial for each tissue.

Such superior results led others to try modifications of Evan's protocol on more types of tissue. Fujiwara and Uehara(22) used a simple HCl treatment, without any collagenase digestion, to study the smooth muscle of monkey mesenteric arteries (Figure 8). Individual VSM cells were exposed, but the contractile state of the media made any assessment of cell shape suspect. The method of Evan et. al.,(18) was the basis for this method, but the authors did not explain why the collagenase II digestion step was eliminated. Fujiwara et. al.,(21) used the simple HCl method to expose the smooth muscle of monkey mesenteric veins. The authors declared that these vessels were preserved in a dilated state because they "were perfused through the heart". The exposed venous VSM cells did not exhibit the severe folding of the cell membrane and the resulting distortions and protrusions demonstrated in a previous study(22) (Figure 9). The cells did mimic the venous walls from vasculatures vasodilated by adenosine ($10^{(-5)}$M) prior to perfusion (Figure 10; see also figures 14-21).(43,66) Holley and Fahim(28) tried a simple HCl treatment to expose portions of the vasculature from skeletal muscle fragments (Figures 11, 12). Their method of fixation was to rapidly expose the muscle of interest and fix the microvessels "in situ by drop-wise application" of phosphate-buffered 2.5% glutaraldehyde. They reported that their method would denude perivascular cells around capillaries and venules. Some of their cell loss probably was due to the greater degree of shrinkage that had occurred within the intima and separated the perivascular cells from the intima. Uehara and Fujiwara(61) used acetylcholine and perfusion at physiological pressure to dilate monkey mesenteric arteries (Figure 13a). Other monkey mesenteric arteries were dissected out of

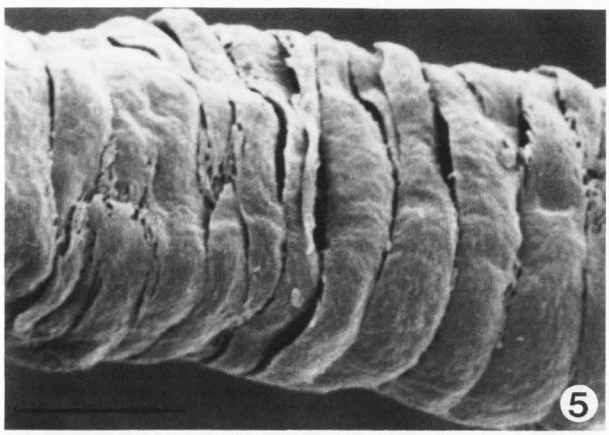

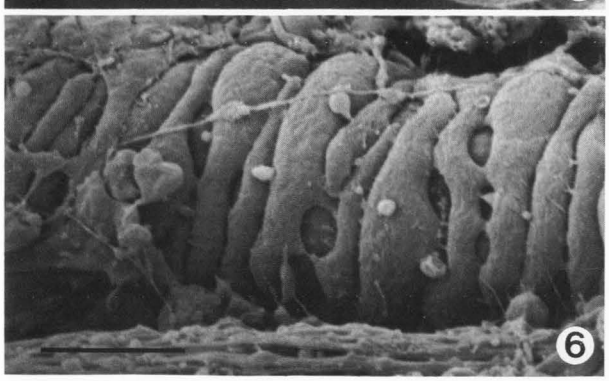

Figure 5. The adventitial aspect of the VSM cells of an arteriole from the hamster cheek pouch treated with the HCl-collagenase after the method of Evan et. al.,(18). VSM cells appeared to be spindle-shaped and were wrapped around their vessel such that the cell's longitudinal axis was about perpendicular to the longitudinal axis of the vessel (ie. parallel to the vessel's radial axis). Bar = 10μm. from: Uehara and Suyama.(62)

Figure 6. The adventitial aspect of VSM cells of the central arteriole in the rat retina, exposed by collagenase and trypsin digestion prior to fixation. Cell shape and orientation were similar to that noted for Figure 5. Note a number of grooves in the sarcolemma. Bar = 10μm. from: Uehara and Suyama.(62)

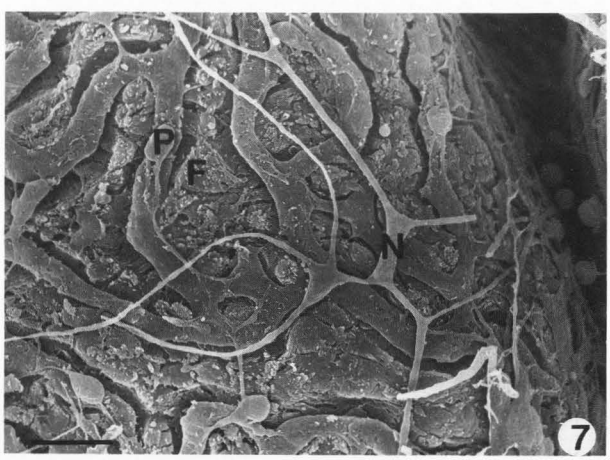

Figure 7. Monkey thyroid gland digested after the method of Evan et. al.,(18). Various components were exposed in addition to blood capillaries: nerve fibers (N), pericytes (P), follicular cells (F). The lymph capillaries were removed during digestion. Bar = 10μm. from: Shimada(54).

their tissue bed and then exposed to norepinephrine in order to induce vasoconstriction (Figure 13b). This study demonstrated that most of the adventitial folds and spherical, ellipsoidal, or bulbous projections frequently associated with normal VSM morphology(22,28) were specifically due to the contracted state of the vascular muscle. Fujiwara and Uehara(23) used the method of Nagato et. al.,(49) to study the cytoarchitecture and innervation pattern of the microvessels in the rat mammary gland by SEM. In brief, tissue blocks were digested with collagenase II and hyaluronidase, fixed with buffered 3% glutaraldehyde, and then hydrolyzed in HCl prior to further preparation for SEM. Using this approach, the authors described the resulting morphology of the VSM cell, pericytes, and perivascular autonomic nerve plexus. (Figure 14). This study was able to precisely localize the perivascular cells to specific sites within the vascular system, from the arteriolar segment through the capillary bed into the muscular venules, while introducing a minimum of identifiable damage or artifact.

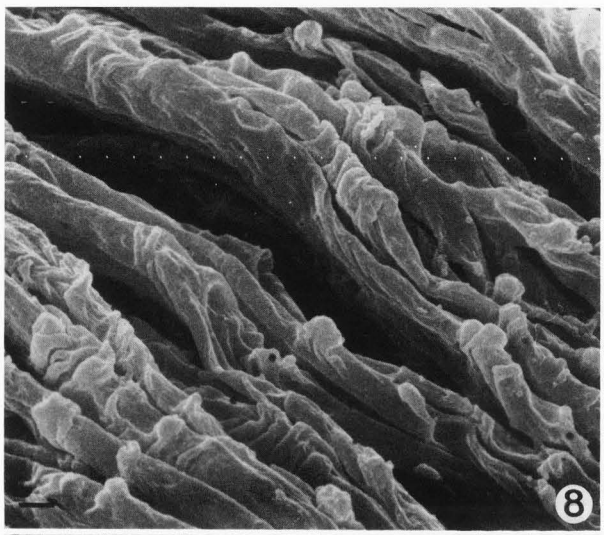

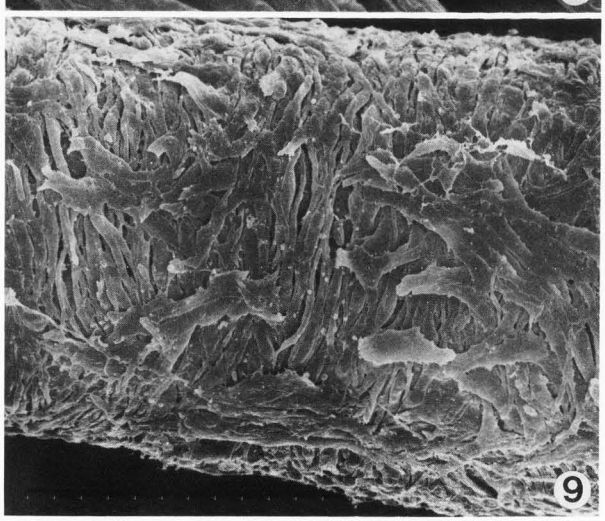

Figure 8. Adventitial aspect of the media of a mesenteric artery in the monkey exposed by a simple HCl method(22). Note the individual VSM cells with extensive nodular protrusions and laminar folds. Bar = 10μm. from: Fujiwara and Uehara.(22)

Figure 9. Adventitial aspect of a mesenteric vein in the monkey exposed by a simple HCl method(22). Note that the VSM cells did not exhibit the nodular protrusions or laminar folds of Figure 8. Bar = 10μm. from: Fujiwara et. al.,(21).

Microdissection and Digestion

These early efforts lead to the approach of exposing vessels by a methodology combining dissection and digestion. Indeed, Evan et. al.,(18) initially suggested this approach because they cubed pieces of tissue (1 cm^2), gently teased apart ganglia, and

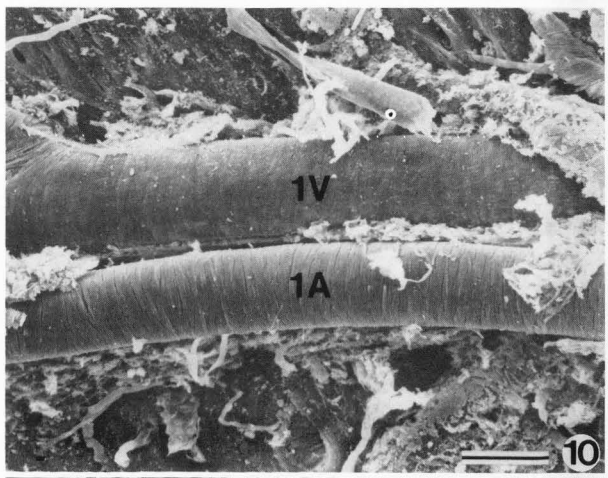

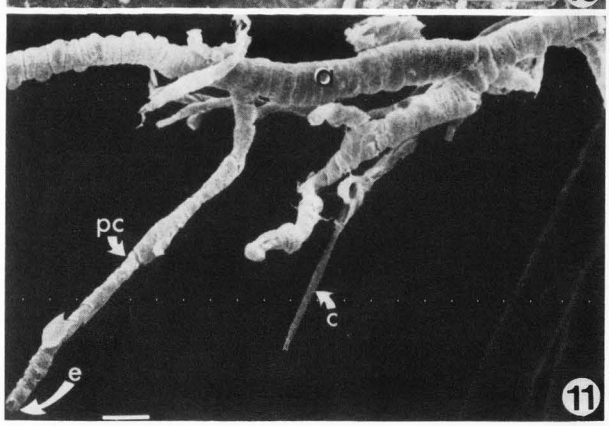

Figure 10. The adventitial aspect of a first-order submucosal arteriole (1A) and venule (1V) in the rat prepared by the method of Miller et. al.,(43). The cells of the venule appeared narrower and thinner when compared to those of its arteriole. Note that neither the venular or arteriolar VSM cells demonstrated any nodular protrusions or laminar folds due to the presence of vascular tone. Bar = 10μm. from: Miller et. al.,(43).

Figure 11. A segment of the microvasculature exposed by a simple HCl treatment(22) from mouse skeletal muscle. Portions of the microvasculature shown: arteriole (a), precapillary arteriole (pc), capillary (c), (e) endothelium. VSM cells were seen wrapping around the arteriole. Bar = 10μm. from: Holley and Fahim.(28)

freed single nephrons by microdissection. These steps isolated specific cells for study and greatly reduced the time of exposure to HCl necessary to completely remove the connective tissue covering the cells of interest. Reducing the time of digestion also limited the amount of damage inflicted on the cells of interest. Mazanet and Franzini-Armstrong(37) noted the same problem of digestion time when using phosphate-buffered trypsin to eliminate components of connective tissue and to expose the pericytes associated with small vessels from the sternomastoid muscle of the rat. If large amounts of collagen had to be removed from the muscle, the pericytes or portions of vessel branches may be lost because of the longer exposure time to HCl. Teasing the muscles into small bundles helped to circumvent this problem.

Miller et. al.,(43) further modified the basic method of Evan et. al.,(18) to study microvessels. The first-, second-, third-, and fourth-order arterioles (1A, 2A, 3A, and 4A, after the classification system of Weideman(66)) in the submucosa of the rat small intestine were chosen for study. The primary modifications were to incorporate microdissection to remove the bulk of the multiple tissue layers (muscularis externa) obscuring the vascular bed within the wall of the small intestine and to reinfuse whole blood into the tissue after perfusion. The lack of reinfused whole blood allowed the vessels to be significantly distorted (Figure 15). Visible connective tissue elements still obscuring microvessels of interest could be further eliminated by additional microdissection immediately over or around the vessel(s) (Figure 16). These dissections were performed to improve the exposure of a variety of different sized microvessels in their natural location with their normal relationship to each other undisturbed. Samples revealed excellent preservation of the three-dimensional organization of the vasculature and the arteriolar wall with minimal damage to the cell membrane (Figure 17). In order for the vasculature to survive handling and processing, Miller et. al.,(43) noted that if whole blood was reinfused into the vasculature after perfusion fixation, the vessels, even the smallest submucosal arterioles and venules, experienced a minimum of

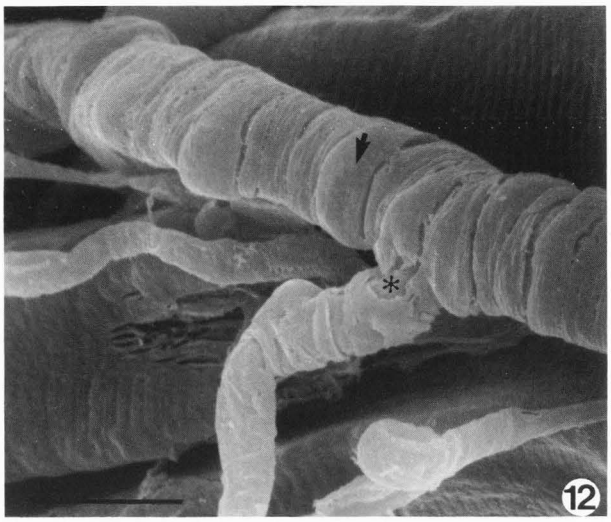

Figure 12. A mouse skeletal muscle arteriole exposed by the simple HCl method(22). VSM cells (arrow) wrap around the intima (asterisk). Bar = 10μm. from: Holley and Fahim.(28)

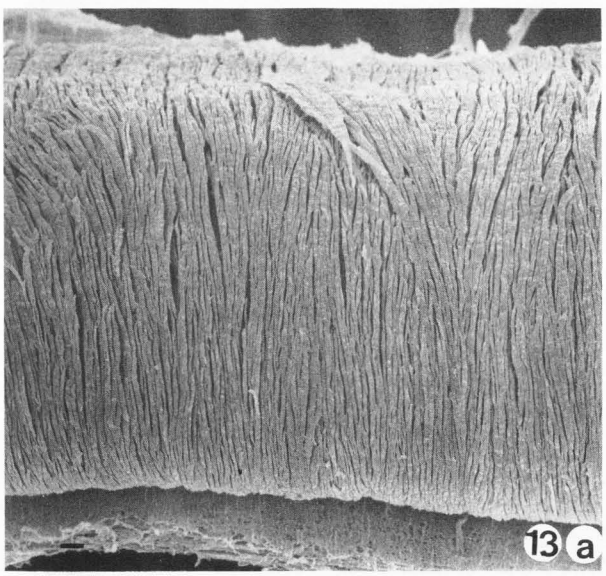

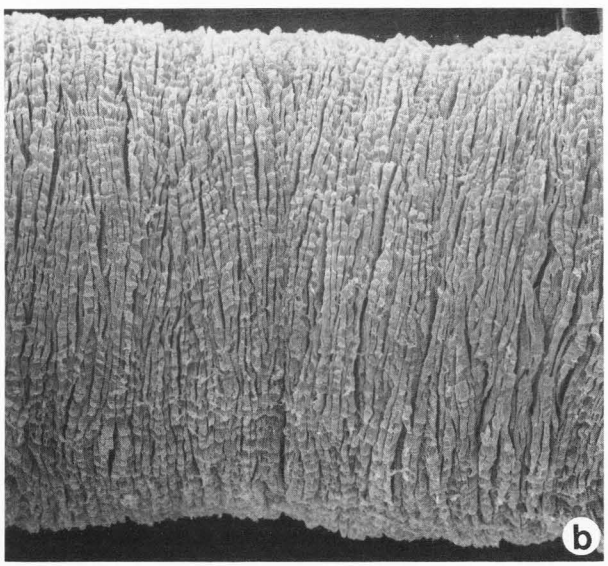

Figure 13. Mesenteric arteries in the monkey exposed by a simple HCl method(22). **a.** The outer (adventitial) aspect of a distended artery. Note that the VSM cells of this vessel segment and of the segment in **b.** are generally oriented perpendicular to the vessel's long axis. Bar = 10μm. **b.** The outer (adventitial) aspect of a constricted artery. The VSM cells of this vessel had a rougher texture because of the nodular protrusions and laminar folds due to its contracted state. However, the muscle cells generally remained fusiform in shape and oriented perpendicular to the vessel's long axis. Bar = 10μm. from: Uehara and Fujiwara.(61)

distortion and damage from handling (Figure 16). Such survival of the vascular system made the monitoring of a single vessel or the precise identification of specific types of vessels possible from the initial harvesting of the tissue into the SEM (Figure 18).

Miller(38) took further advantage of reinfusing the vasculature to study the entire circumference of first-, second-, and third-order submucosal arterioles. He found that vessel segments, identified *in situ* by LM after drying by the critical point method, could be singled out and, if still partially obscured, further dissected to complete exposure. At this point, it became obvious that microvessels could be completely removed from their *in situ* position (mobilized), retrieved with the aid of a microprobe, and remounted onto a SEM specimen holder. By remounting the vessel segments "end-on" and placing the specimen holder into a SEM with a goniometer stage, sequential photographs could be made around each vessel as it was rotated on its longitudinal axis. Thus, the entire circumference of a vessel could be recorded (Figure 19).

SEM analysis of these arterioles confirmed that their media consists of a monolayer of VSM cells. The largest arterioles that were paired with a large venule were called 1st-order arterioles (1A). Further branchings that also separated an arteriole from its companion venule produced the microvessels termed 2nd-order arterioles (2A). The 3rd-order arterioles (3A) were those formed at approximately a right angle when the next branching occurred. The only variation from this fact noted within the submucosal arterial system was found along the largest submucosal arterioles (1A) that connect directly to the mesenteric arterial vessels supplying the intestine.(43,38) When these continuations of the mesenteric arteries penetrate the muscularis externa of the small intestine, they have approximately two layers of VSM cells. As one progresses distally from the point of penetration, the number of vascular muscle layers rapidly decreases to a monolayer. The media in arterioles of similar diameters in other tissue beds also have been shown to consist of a monolayer of vascular muscle.(11-13,23,25,26,28,45,62)

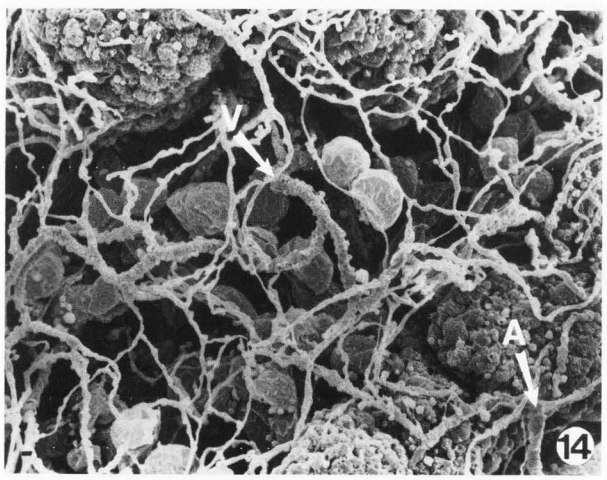

Figure 14. SEM micrograph showing a microvascular network exposed in the interacinal space of the rat mammary gland. The pathway of the vessels could be followed from the arteriolar (A) to the venular (V) side via a capillary bed. Exposure was accomplished by the collagenase II-hyaluronidase digestion method of Nagato et. al.,(49). Bar = 10μm. from: Fujiwara and Uehara.(23)

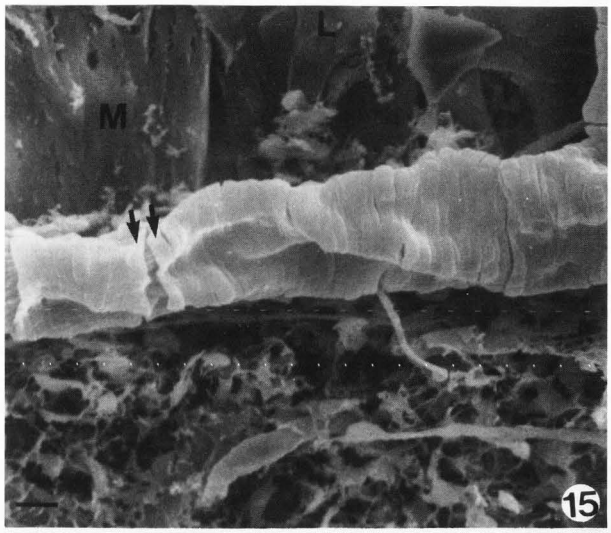

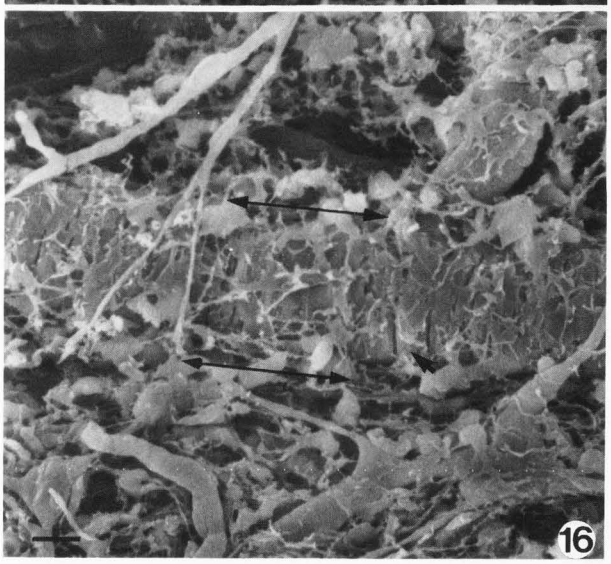

Figure 15. SEM micrograph of a submucosal arteriole that was processed by the method of Miller et. al.,(43), except that whole blood was not reinfused into the vasculature after fixation. Individual VSM cells (arrows) were clearly exposed and easily seen. However, the vessel collapsed, causing much distortion and the separation of many cells (between arrows). Lymphatic vessel (L), muscularis mucosa (M). Bar = 10μm. from: Miller et. al.,(43).

Figure 16. SEM micrograph of a submucosal arteriole (between 2-headed arrows) from a sample of small intestine in the rat. This sample was processed by the method of Miller et. al.,(43), except that no digestion was performed. Connective tissue elements still partially obscured many individual vessels in that their VSM cells (arrow) were not completely visible. Bar = 10μm. from: Miller et. al.,(43).

Other studies have used the basic method of Miller et. al.,(43) to study the cerebral vascular systems of rat and dog. Moore et. al.,(45) studied the VSM of cerebral arterioles in adult rats after 4 weeks of exposure to streptozotocin-induced hyperglycemia (435-596 mg/dl). The authors substituted paraformaldehyde and a brief dip into 8N HCl for, respectively, the perfusion fixative and the 5M potassium hydroxide (KOH) treatment of the method of Miller et. al.,(43). Many diabetic VSM cells had changed from the normal spindle shape to a branched or stellate configuration (Figure 20). Concurrent TEM analysis demonstrated endothelial cell necrosis in most vessels and intracellular abnormalities within the VSM cells. Shiraishi et. al.,(55) studied the architecture of the media of cerebral blood vessels from mongrel dogs. The authors sacrificed the animals by perfusion through the heart with saline, followed by phosphate-buffered 3% glutaraldehyde and heparinized whole blood. A constant pressure of 120 mmHg was maintained during the perfusion and reinfusion of whole blood. After removing the entire brain, pieces of brain approximately 5x5x5 mm in size were taken from selected areas. Ultrasonic treatment was used to loosen the smaller vessels from surrounding tissues. Larger vessels were mechanically lifted from the fixed brain. Specimens were rinsed in buffer and postfixed with OsO_4. This latter step allowed the visualization of the unstained, and therefore white, connective tissue that covered the vessel. At this point, the specimens were treated with 8 N HCl for 20-30 minutes at 60°C, until the vessels, blackened with OsO_4, could be seen under a dissecting microscope. The authors showed the presence of multiple layers of spindle-shaped VSM cells. The authors also described " 'asteroid-like' muscle cells", which were regarded as "deformed longitudinal muscle cells", and longitudinally-oriented VSM cells (Figure 21). The "circular muscle cells" of the various arteries were described as follows: the "arteries" (>100 um outer diameter) had VSM cells 70-120 mm in length and 3.0-5.5 um in maximum width, the "muscular arterioles" (30-100 μm outer diameter) and "terminal arterioles" (10-30 μm

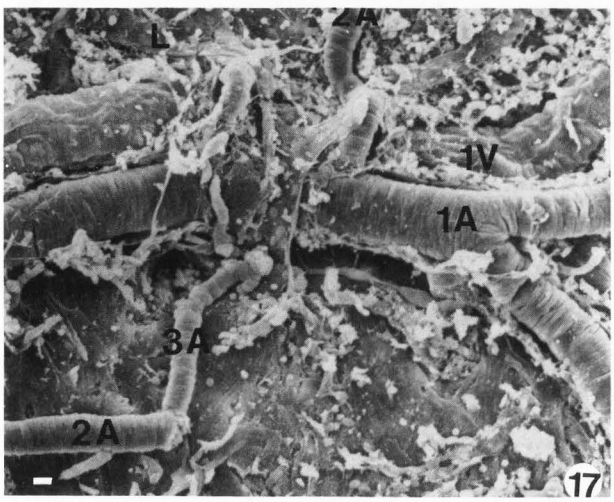

Figure 17. A sample of the submucosal microvasculature in the rat exposed in situ by the method of Miller et. al.,(43). Different types of microvessels were easily seen: first-order (1A), second-order (2A), third-order (3A) arterioles, first-order venule (1V), lymphatic vessels (L). Bar = 10μm. from: Miller et. al.,(42).

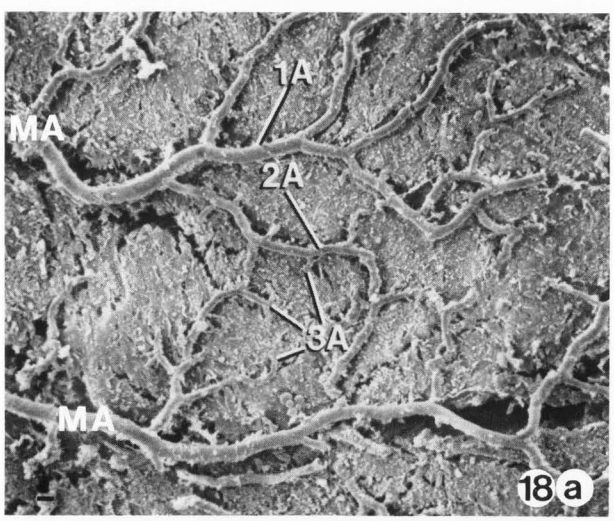

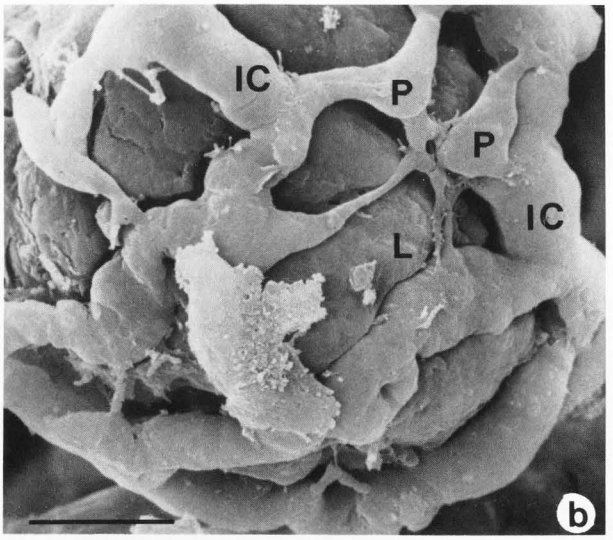

Figure 18. a. A low magnification SEM of the microvascular bed of the small intestine in the rat after being exposed by the method of Miller et. al.,(43) and dried by the critical point method. The two largest arterioles were continuations of the mesenteric arteries (MA) that initially penetrated into the submucosa. Other arterioles of these arcades were prominent (1A, 2A, 3A). Note that the arcades were continuous from their inception to their entry into the mucosa as central arteriole(s). Bar = 10μm. **b.** High magnification SEM of the abluminal aspect of the crypt of Lieberkühn (L) exposed by the method of Miller(38). Islanded capillaries(51) (IC) formed a network coursing over the base of each crypt. Note the pericyte-like cells (P) associated with one or more islanded capillaries. Bar = 10μm. **18a.** from Miller et. al.,(41). **18b.** from Miller.(38)

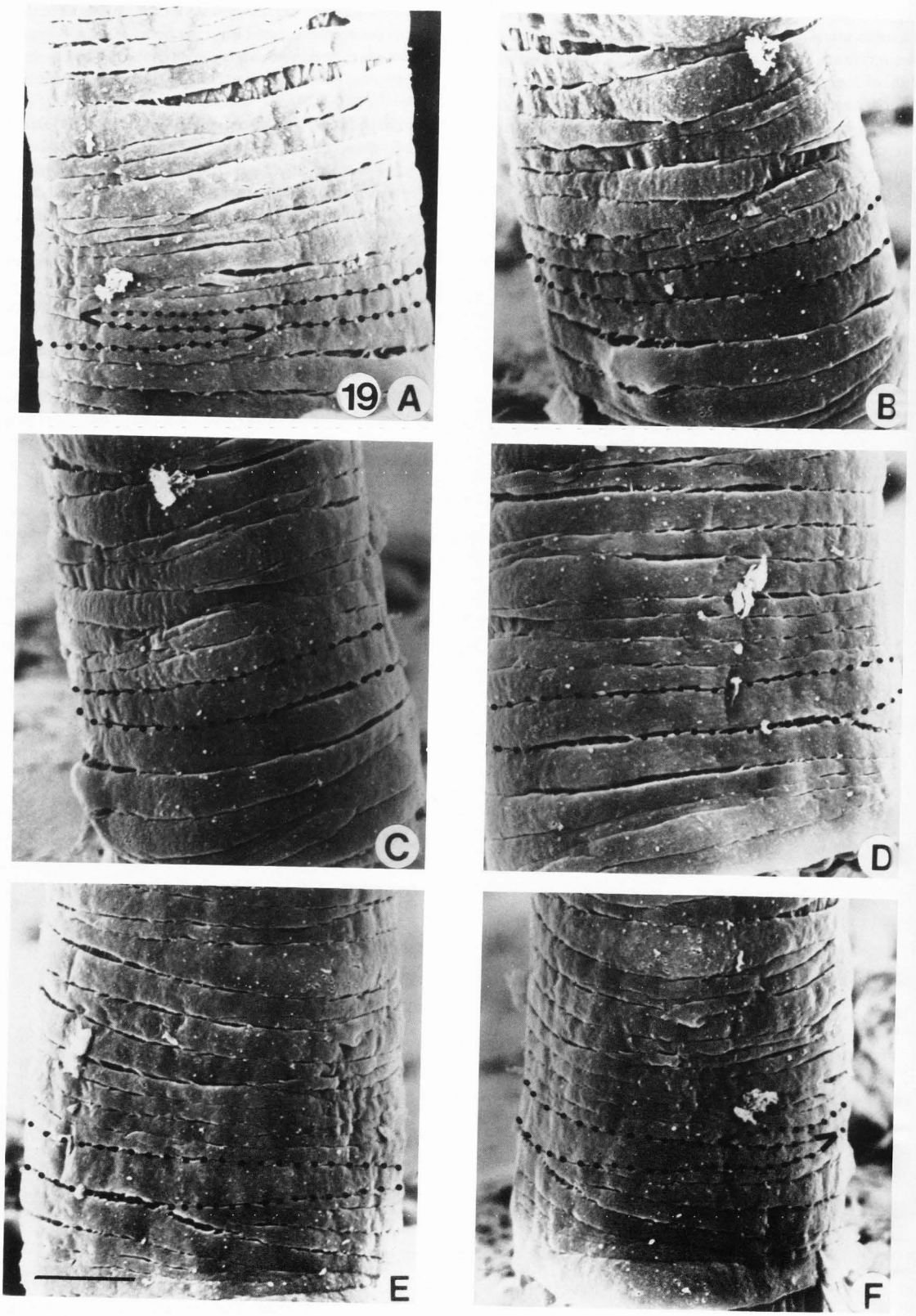

Figure 19. A 2A vessel from a rat submucosa that was exposed by the method of Miller et. al.,(43). The complete circumference could be seen as one progresses from panel 19A to 19F. One VSM cell was outlined (dotted lines) throughout the sequential views. The termination of the two lateral processes were marked (<>). Bar = 10μm. from: Miller et. al.,(42).

outer diameter) had cells 40-50 μm in length and 3-4 μm in maximum width, and the "precapillary arterioles" (outer diameter of about 15 μm) had cells that had three or more branches (ie. lateral processes) were 20-30 μm in length, and 4-6 μm in maximum width.

Miller et. al.,(42) used the method of Miller(38) to completely mobilize, remount, and circumferentially view vessel segments of intestinal submucosal arterioles in Wistar-Kyoto rats (WKY) at 6-8 weeks and 10-12 weeks of age. This method allowed the structural characteristics of first-, second-, and third-order arterioles to be defined. The following measurements were made: 1) outer diameter, 2) number of revolutions each VSM cell made around the vessel, 3) number of VSM cells occupying a length of vessel, 4) the length of individual VSM cells, and 5) the width of lateral processes along their length. All VSM cells had exactly two lateral processes, except for those precapillary arterioles giving rise to or actually being the central arteriole of the mucosal villi (Figure 22). At a given age, the average length and width of the VSM cell was similar for all types of arterioles, from the largest (1A) to the smallest (3A) diameter vessels. The average length and width of the VSM cell and the outer diameter of a particular type of arteriole increased uniformly for all arterioles with age. The younger VSM cells averaged 82-90 μm in length and 3.0-3.5 μm in maximum width. The older VSM cells averaged 101-109 μm in length and 3.5-4.0 μm in maximum width. The authors noted that these data suggested 1) a common population of VSM cells at a given age in terms of length, width, and process morphology and 2) juvenile maturation was associated with a uniform hypertrophy of arteriolar smooth muscle.

Miller et. al.,(41) presented a simplified method to directly determine the average cell length and width per vessel segment using only a single view of a microvessel. This methodology allows quantitative evaluation of VSM cells without the more difficult and tedious necessity of removing and circumferentially viewing the vessel of interest. In order to test this simplified (single view) methodology, it was first necessary to determine the average cell dimensions per vessel segment via circumferential views. Previous work(55) had shown how to determine cell lengths. A method of treating the cells as a series of adjacent trapezoids was used to determine the average cell width (parallel to the vessel's long axis). The details of the mathematical model for the single view method are given in the Appendix of the reference.(55) Figure 23 summarizes the technique used to determine the average width of a cell that was not a simple geometric shape wrapped around a cylinder. The authors also used a computer-assisted image analysis software system to perform the morphometric measurements. The agreement of data obtained from the single view method and the circumferential view method over a wide variety of vessel types was excellent. This single view method has several advantages, which include 1) less handling of the tissue, 2) the capacity of in situ analysis, and 3) the ability to study large numbers of microvessels from a single tissue sample in a short period of time.

Gattone et. al.,(26) proposed an alternative technique for obtaining the average number of wraps per VSM cell (i.e., average number of revolutions a cell made around the vessel) using one view of a microvessel (single view), rather than either the circumferential view(38,55) or the single view(41) of Miller and others. From the average number of wraps per cell, one can calculate the average cell length and width per vessel. Gattone et. al.,(26) tested this technique against the method of Miller(41).(27) The results were in good agreement. Indeed, the mathematical models of Gattone et. al.,(26) and Miller

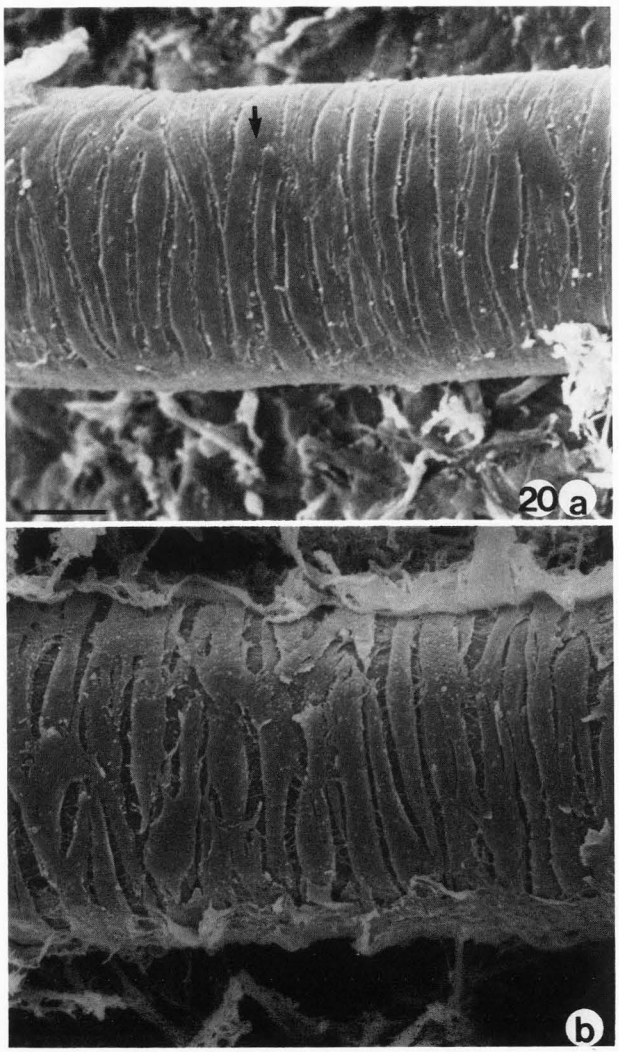

Figure 20. **a.** A control 2A vessel from the cerebral microvasculature in the rat which was exposed after the method of Miller et. al.,(43). Note the uniformity in shape and orientation of the VSM cells (arrow). Bar = 10μm. **b.** A diabetic 2A from the same study. Many irregular to stellate shaped VSM cells were evident. Bar = 10μm. from: Moore et. al.,(45).

et. al.,(41) were of different etiology, but employed the same cellular characteristics to determine the cellular dimensions. One noteworthy aspect of the method of Gattone et. al.,(26) was the ease with which it could be performed by hand without the assistance of a computer.

Miller et. al.,(39) employed their methodologies of mobilizing and circumferentially analyzing microvessels to analyze the submucosal arteriolar VSM from age-matched WKY and spontaneously hypertensive rats (SHR) during the period of life from pre-hypertensive (4-6 weeks) to well developed hypertension (18-20 weeks). First, second-, and third-order arterioles (1A, 2A, and 3A) from all animals demonstrated the normal spindle-shape for VSM cells and the comparable elongation and widening of these cells associated with maturation (Figure 24). VSM cells from young WKY averaged 80-82 μm in length and 1.9-2.0 μm in average width. The VSM cells from adult WKY averaged 84-89 μm in length and 2.0-2.1 μm in average width. VSM cells from young SHR averaged 81-92 μm in length and 1.6-2.0 μm in average width. The VSM cells from adult SHR averaged 84-95 μm in length and 1.8-1.9 μm in average width. The only significant difference shown between the arteriolar VSM cells of WKY and SHR for comparable arteriolar branches was a radial thickening of the muscle cells (parallel to the vessel's radial axis) in the largest arterioles (1A). The smaller arterioles (2A and 3A) studied in the SHR retained a normal VSM cell and overall wall morphology. There was no evidence of any hyperplasia in any type of arteriole. These data suggested that there must be either more than one way that different vessels adapt to hypertensive distension forces or different ways that the genetic expression of hypertension may occur within the intestinal vasculature.

Current Applications

Miller et. al.,(40) have defined morphometric measurements that were used to quantitatively indicate the "normal VSM shape" and describe the alterations in shape detected in Wistar-fatty diabetic rat litters. This rat model produced litter mates who were either normoglycemic (Fa/Fa) or spontaneously became mildly diabetic (blood glucose= 262 ± 36 ml/dl) by 10 weeks of age (fa/fa). The meterics used to quantitate "VSM

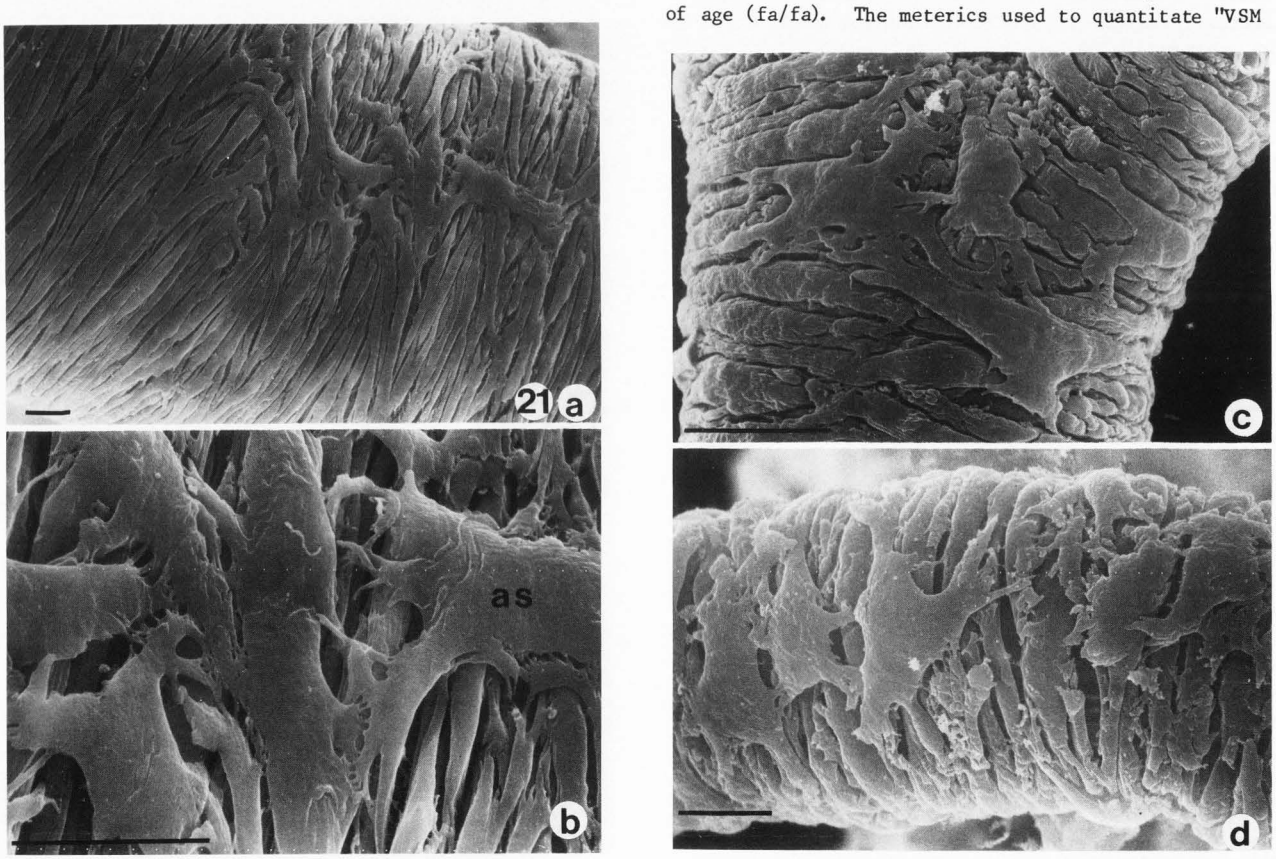

Figure 21. The adventitial aspect of arterial vessels supplied by the middle cerebral artery in the dog, exposed after the method of Miller et. al.,(43). **a.** A portion of a muscular vessel consisting of 2-3 layers of VSM cells. Note the presence of muscle cells coursing over the media in a more longitudinal orientation than the majority of VSM cells. Bar = 10μm. **b.** Several muscle cells showing an "asteroid-like" shape (as) with striations and more than two lateral processes. Bar = 10μm. **c.** An example of the branched portion of an arteriole 10-30 μm in outer diameter. The majority of VSM cells were spindle-shaped cells oriented perpendicular to the long axis of the vessel. Note the presence of muscle cells having irregular shapes. Bar = 10μm. **d.** An unbranched portion of an arteriole 10-30 μm in outer diameter. Several "asteroid-like" VSM cells appeared to lie over more uniform muscle cells. from: Shiraishi et. al.,(55).

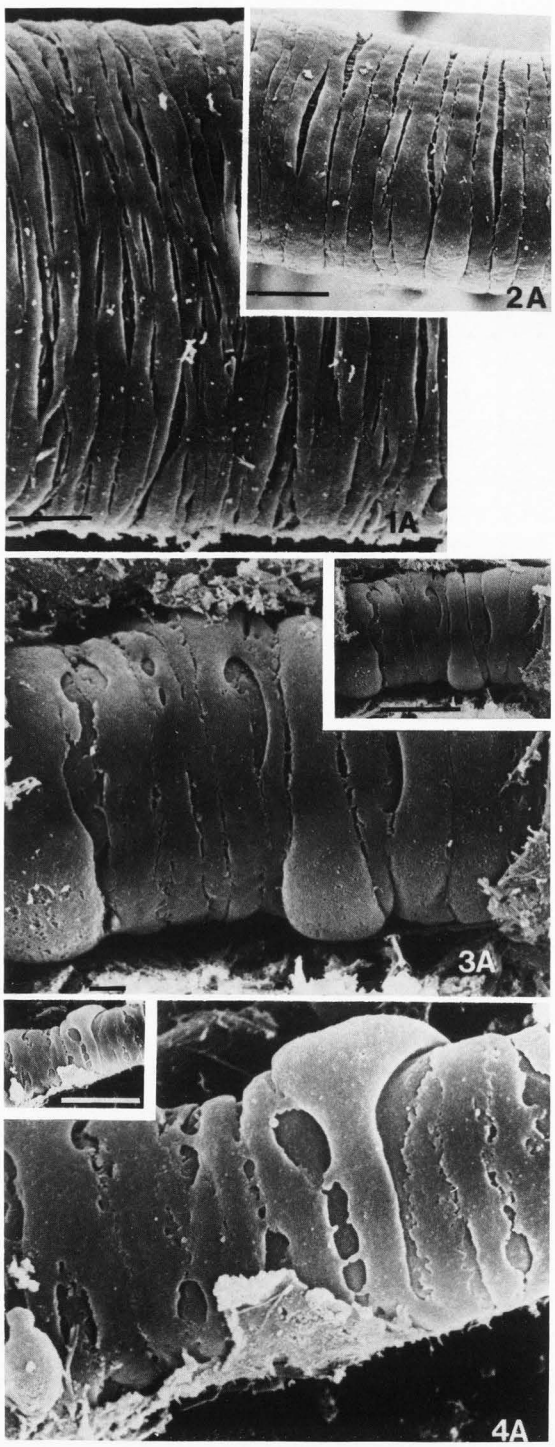

Figure 22. Examples of the submucosal arterioles in the rat, exposed by the method of Miller et. al.,(43). Note the VSM cells were a monolayer that was usually spindle shaped and oriented perpendicular to the vessel's long axis. 1A, 2A, and the 3A and 4A inserts are the same magnification. Note that the VSM cells became more irregular in shape and began to suggest that their lateral processes could be branched. Bars = 10μm. from: Miller et. al.,(42).

shape" were as follows: 1) the average VSM cell length, 2) the average cell width, 3) the average ratio of cell length-to-width (Lc/Wc), 4) the number of average lateral processes per VSM cell (LP/VSM), 5) the average number of "misplaced" somal enlargement regions per the total number of VSM cells (CB/TNC), 6) the average number of lateral processes per the total number of VSM cells that overlap another cell (XC/TNC), and 7) the average number of VSM cells per the total number of cells whose external shape could not be scored as fusiform (ODD/TNC). This type of quantitation is needed so that age, organ, or disease related differences in morphology can be identified. The impetus for such information was provided because Moore, et. al.,(45) had noted dramatic qualitative changes in the cerebral arteriolar VSM after only 4 weeks of STZ-induced hyperglycemia. Our preliminary analysis of the intestinal microvessels, after 12 weeks of mild hyperglycemia, noted definite alterations in morphology. The alterations are best described by the examples presented in Figure 25.

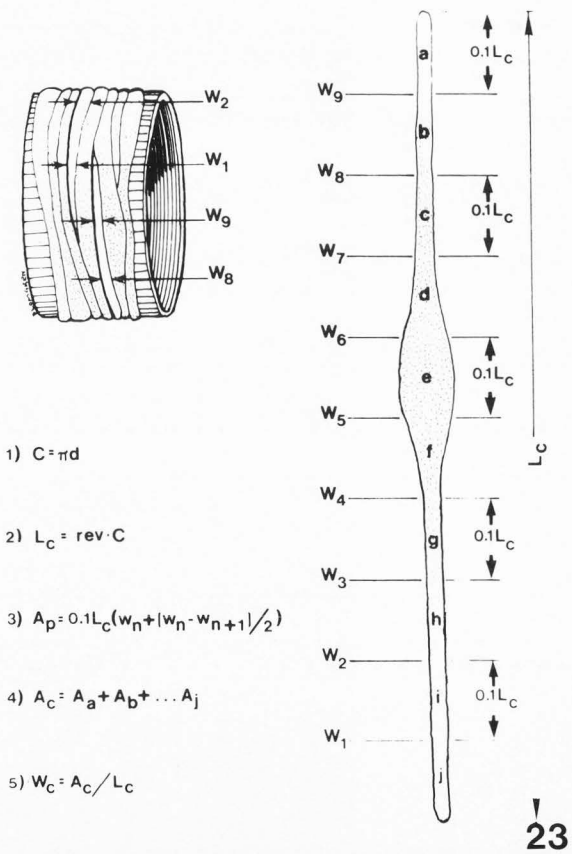

Figure 23. An illustration showing how the average VSM cell width was obtained from circumferentially viewed cells. Lines 1-9 depicted the location where measurements were made. The length between each width measurement was about $0.1L_c$. The above measurements were used to calculate the area of each quadrangular cell portion (a-j). The mean width of a VSM cell (W_c) was calculated by dividing the total cell area (A_c) by the total length (L_c) of the cell ($W_c = a_c/L_c$). from: Miller et. al.,(41).

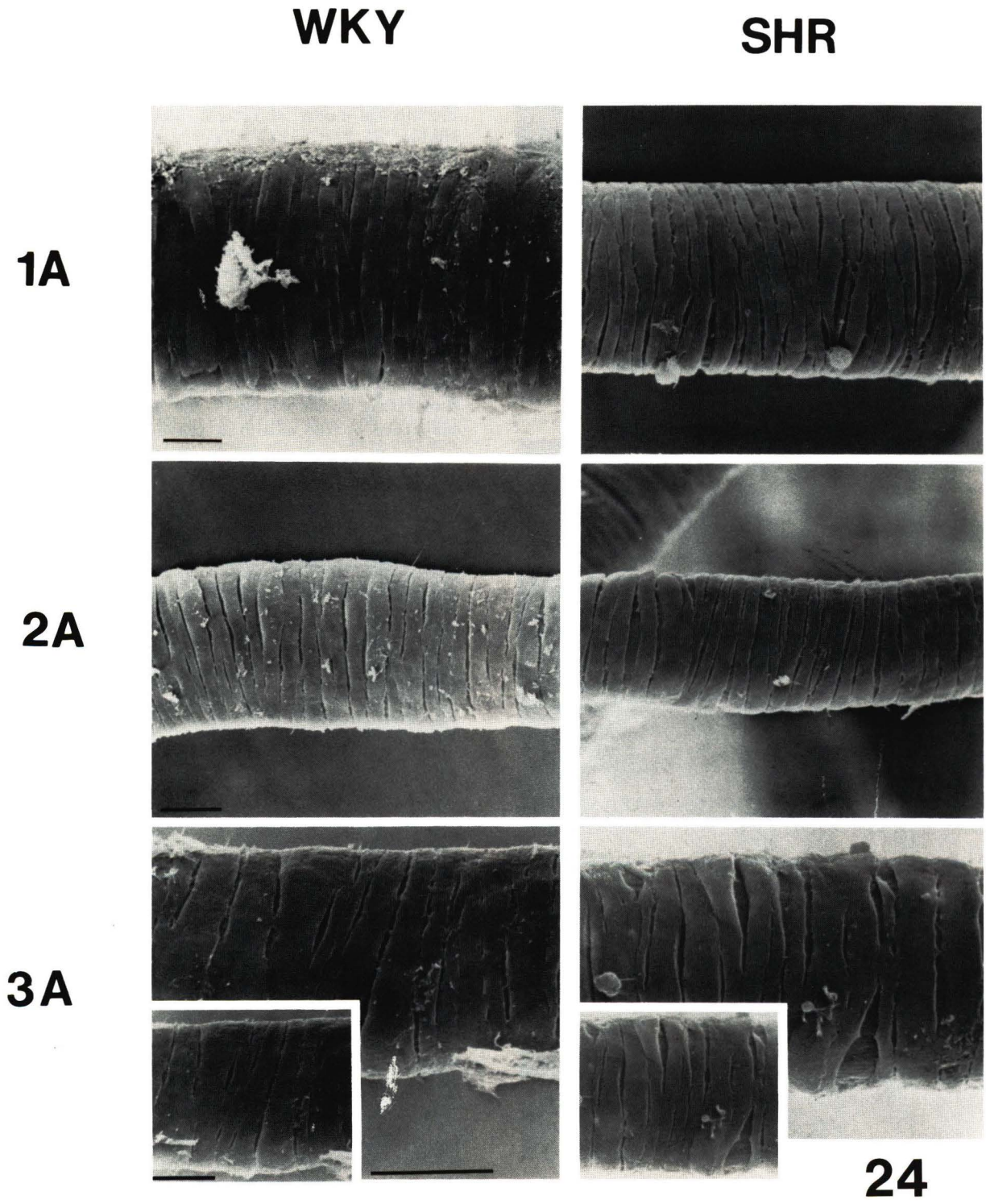

Figure 24. SEM micrographs representative of all the 1A, 2A, and 3A from adult WKY and SHR. These SEM views also were representative of the young WKY and SHR. Note the spindle-shape of all VSM cells, that the VSM cells were oriented almost perpendicular to the vessel's long axis, and that the monolayer of muscle cells did not overlap. Bars = 10μm. from: Miller et. al.,(40).

Some VSM cells had their somal enlargement region expanded parallel to the vessel's longitudinal axis. This expansion would even cross over one or more neighboring cells. Other cells exhibited an apparent increase in the number of lateral processes. The mechanism of these alterations has not been determined as of this review. Two possible mechanisms for the increased number of lateral processes are an actual intracellular reorganization to induce this phenomenon or the fusion of all or part of two or more cells which would produce this alteration. As we encounter more of these changes, we shall be able to better elucidate their causes. Subtle differences in the quantitative description of VSM morphology were noted between the three types of animals. However, we have not completed our statistical analysis. Thus, the final evaluation and interpretation of results await completion. Through careful collection and analysis of the data from these three types of animals for VSM cells in different types of arterioles, we shall be able to determine what effect abnormal morphology, such as cell body expansion, extra lateral processes, or the two in combination, has on the ability to quantitatively describe such changes in VSM cell shape.

Summary

The usefulness of SEM for analyzing the walls of the vascular system has been demonstrated by numerous investigators. There are several methodologies available for exposing not only the VSM cells, but also other types of tissue or structures associated with the vasculature, such as the basal surface of endothelium, pericytes, adventitial tissues, or nerve fibers. Various combinations of procedures have been used to improve the exposure, selection, and preservation of perivascular and vascular structures. Chemical and enzymatic digestion steps will continue to be the principal elements of any methodology for exposing structures normally obscured by in vivo tissue components. The combination of microdissection, prior to processing the specimen for SEM, with digestion has allowed better preservation of the tissues by reducing the amount of material obscuring the tissues of interest. This additional microdissection, in turn, decreased the length of time needed by the digestion solution(s) to successfully expose the target tissues. Using microdissection after drying by the critical point method has allowed the complete mobilization of vessels from their location in situ for detailed analysis of the entire circumference. The ability to analyze cell morphology means that individual VSM cells from a precisely localized portion of the vasculature can be described. Such quantitation will allow accurate descriptions of the morphological changes caused by normal events (i.e., aging, contraction) and pathological conditions. As more investigators utilize the various methodologies for exposing the vasculature, our ability to expose other selected perivascular structures and portions of the vasculature will only improve with time.

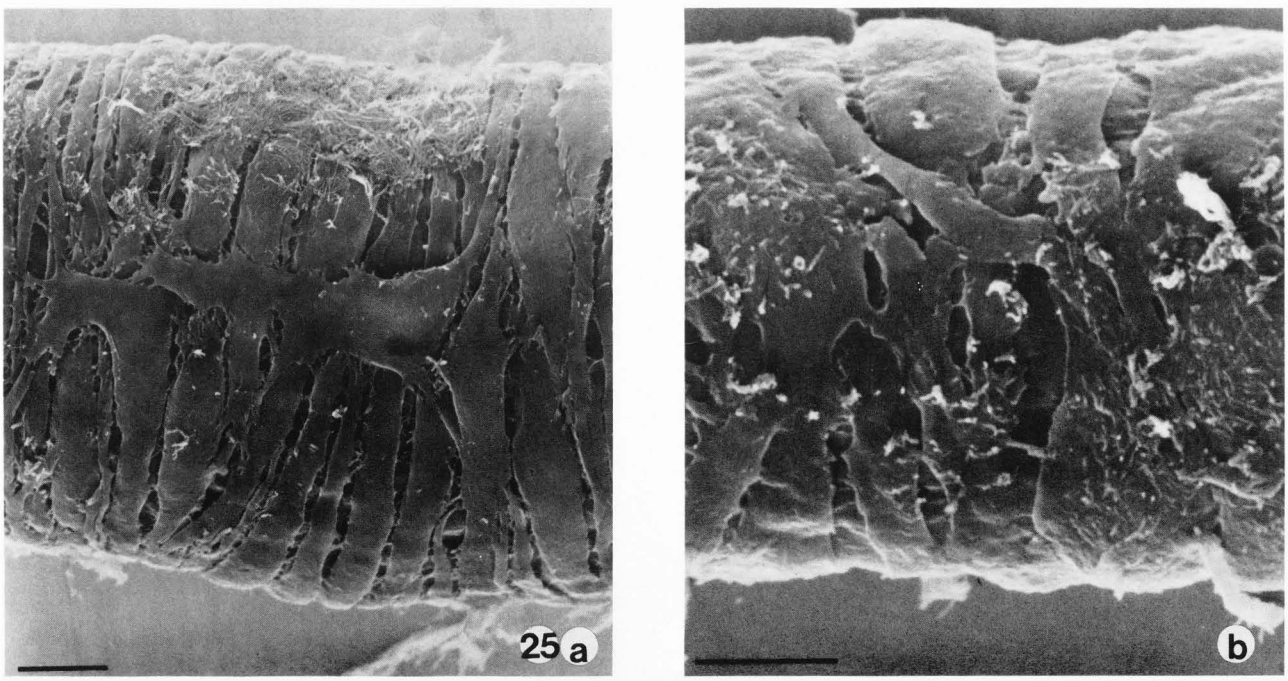

Figure 25. SEM micrographs of intestinal arterioles from the WKY-fatty rat model of spontaneous diabetes. **a.** The monolayer of VSM in a 1A. Note the longitudinal expansion of several muscle cells which crossed over adjacent cell(s). Bar = 10μm. **b.** The VSM cells in a 2A. The lateral process of one cell has crossed over its neighbor. The lateral process of another muscle cell had apparently split in two, resulting in three processes, not the normal number of two. Bar = 10μm. from: Miller et. al.,(40).

Acknowledgements

This study was funded in part through the National Institute of Health PHS Grants HL-20605 and HL-25824 and the NIH Career Development Award HL-1089 presented to Dr. H. Glenn Bohlen, Department of Physiology and Biophysics, Indiana University School of Medicine, Indianapolis, Indiana. We wish to thank Philip Blomgren, Patrica Summerlin, and Julie Goldman for their technical help.

References

1. Aherne WA, Dunhill MD. (1982). Methods of estimating myofiber size. In: Morphometry, Edward Arnold (Publishers) Ltd., London, p. 103.

2. Anderson TF. (1951). Techniques for the preservation of three-dimensional structure in preparing specimens for the electron microscope. Trans. N.Y. Acad. Sci. 13:130-134.

3. Auer LM, Johansson BB. (1980). Dilatation of pial vessels in hypercapnia and in acute hypertension. Acta Physiol. Scand. 109:249-251.

4. Bohlen HG, Gore RW. (1976). Preparation of rat intestinal muscle and mucosa for quantitative microcirculatory studies. Microvas. Res. 11:103-110.

5. Bohlen HG, Gore RW. (1977). Comparison of microvascular pressures and diameters in the innervated and denervated rat intestine. Microvas. Res. 14:251-264.

6. Bohlen HG, Gore RW, Hutchins PM. (1977). Comparison of microvascular pressures in normal and spontaneously hypertensive rats. Microvas. Res. 13:125-130.

7. Bohlen HG, Hankins KD. (1982). Early arteriolar and capillary changes in streptozotocin-induced diabetic rats and intraperitoneal hyperglycaemic rats. Diabetologia 22:344-348.

8. Bohlen HG, Lobach D. (1978). In vivo study of microvascular wall characteristics and resting control in young and mature spontaneously hypertensive rats. Blood Vessels 15:322-330.

9. Bohlen HG, Niggl BA. (1980). Early arteriolar disturbances following streptozotocin-induced diabetes mellitus in adult mice. Microvas. Res. 20:19-29.

10. Boyde A, Wood C. (1969). Preparation of animal tissues for surface-scanning electron microscopy. J. Microsc. 90:221-249.

11. Castenholz A. (1980). Scanning electron microscopy of myocytes and pericytes in corrosion casts in terminal blood vessels of the rat. Microvasc. Res. 19:395.

12. Castenholz A. (1983). Visualization of periendothelial cells in arterioles and capillaries by scanning electron microscopy of ultrasound treated and plastoid injected brains in rats. Scanning Electron Microsc.1983; I:161-170.

13. Castenholz A, Zöltzer H, Erhardt H. (1982). Structures imitating myocytes and pericytes in corrosion casts of terminal vessels. A methodical approach to the phenomenon of "plastic strips" in SEM. (abstract) Mikroscopie Wein 39:95-106.

14. Cohen AL, Marlow DP, Garner GE. (1968). A rapid critical point method using fluorocarbons ("Freons") as intermediate and transitional fluids. J. de Microsc. (Paris) 7:331-342.

15. Cope DA, Roach MR. (1975). A scanning electron microscopic study of human cerebral arteries. Can. J. Physiol. 53:651-659.

16. Cox RH. (1981). Basis for the altered arterial wall mechanics in the spontaneously hypertensive rats. Hypertension 3(4):485-495.

17. Dyck PJ, Lais AC. (1970). Electron microscopy of teased nerve fibers: method permitting examination of repeating structures of same fiber. Brain Res. 23:418-423.

18. Evan AP, Dail WG, Dammrose D, Palmer C. (1976). Scanning electron microscopy of cell surfaces following removal of extracellular material. Anat. Rec. 185:433-446.

19. Finlay JB, Hunter JAA, Steven FS. (1971). Preparation of human skin for high resolution scanning electron microscopy using phosphate-buffered crude bacterial a-amylase. J. Microsc.93:73-84.

20. Friedman SM, Nakashima M, Mar MA. (1971). Morphological assessment of vasoconstriction and vascular hypertrophy in sustained hypertension in the rat. Microvas. Res. 3:416-425.

21. Fujiwara T, Ikeuchi M, Uehara Y. (1983) Scanning electron microscope study of smooth muscle cells in the mesenteric veins of the monkey. Biomed. Res. 4:225-230.

22. Fujiwara T, Uehara Y. (1982). Scanning electron microscopical study of vascular smooth muscle cells in the mesenteric vessels of the monkey: Arterial smooth muscle cells. Biomed. Res. 3:649-658.

23. Fujiwara T, Uehara Y. (1984). The cytoarchitecture of the wall and the innervation pattern of the microvessels in the rat mammary gland: A scanning electron microscopic observation. Am. J. Anat. 170:39-54.

24. Furuyama M. (1962). Histometrical investigations of arteries in reference to arterial hypertension. Tohoku J. Exper. Med. 76:388-414.

25. Gattone II, VH, Luft FC, Evan AP. (1984). The renal afferent and efferent arterioles of the rabbit. Am. J. Physiol. 247:F219-228.

26. Gattone II, VH, Fineberg NS, Evan AP. (1985). A proposed technique for the morphometric analysis of arteriolar smooth muscle cells from scanning electron microscopic preparations. J. Submicrosc. Cytol. 17:551-554.

27. Gattone II, VH, Miller BG, Evan AP. (1986). Microvascular smooth muscle cell quantitation from scanning electron microscopic preparations. Anat. Rec. 216:443-447.

28. Holley JA, Fahim MA. (1983). Scanning electron microscopy of mouse microvasculature. Anat. Rec. 205:109-117.

29. Hua C, Cragg B. (1980). Measurements of smooth muscle cells in arterioles of guinea pig ileum. Acta Anat. 107:224-230.

30. Joyner WL, Davis MJ, Gilmore JP. (1981). Intravascular pressure distribution and dimensional analysis of microvessels in hamsters with renovascular hypertension. Microvas. Res. 22:190-198.

31. Komuro T, Desaki J, Uehara Y. (1982). Three-dimensional organization of smooth muscle cells in blood vessels in laboratory rodents. Cell Tissue Res. 227:229-237.

32. Lee RMKW. (1985). Vascular changes at the prehypertensive phase in the mesenteric arteries from spontaneously hypertensive rats. Blood Vessels 22:105-126.

33. Lee RMKW, Forrest JB, Garfield RE, Daniel EE. (1983). Comparison of blood vessel wall dimensions in normotensive and hypertensive rats by histometric and morphometric methods. Blood Vessels 20:245-254.

34. Lee RMKW, Garfield RE, Forrest JB, Daniel EE. (1983). Ultrastructural changes in mesenteric arteries from spontaneously hypertensive rats. Blood Vessels 20:72-91.

35. Lee RMKW, Garfield RE, Forrest JB, Daniel EE. (1983). Morphometric study of structural changes in the mesenteric blood vessels of spontaneously hypertensive rats. Blood Vessels 20:57-71.

36. Limas C, Westrum B, Limas CJ. (1980). The evolution of vascular changes in the spontaneously hypertensive rat. Am. J. Pathol.98:357-384.

37. Mazanet R, Franzini-Armstrong C. (1982). Scanning electron microscopy of pericytes in rat red muscle. Microvas. Res. 23:361-369.

38. Miller BG. (1984). Structural characteristics of the arteriolar smooth muscle cells in the small intestine of the rat. Ph.D. thesis, Indiana University School of Medicine, Reg. no. TX-1-547-564, pp.47,48,89,90.

39. Miller BG, Connors BA, Bohlen HG, Evan AP. (1987). Cell and wall morphology of intestinal arterioles from 4- to 6- and 17- to 19-week-old Wistar-Kyoto and spontaneously hypertensive rats. Hypertension 9:59-68,

40. Miller BG, Evan AP, Bohlen AP. (1987). Quantitating the "shape" of vascular smooth muscle cells (VSM) from WKY & spontaneously diabetic rats. Fed. Proc. 46:(M100)1536.

41. Miller BG, Gattone II, VH, Overhage JM, Bohlen HG, Evan AP. (1986). Morphological evaluation of vascular smooth muscle cell: Length and width from a single scanning electron microscopic micrograph of microvessels. Anat. Rec. 216:95-103.

42. Miller BG, Overhage JM, Bohlen HG, Evan AP. (1985). Hypertrophy of arteriolar smooth muscle cells in the rat small intestine during maturation. Microvasc. Res. 29:56-69.

43. Miller BG, Woods RI, Bohlen HG, Evan AP. (1982). A new morphological procedure for viewing microvessels: A scanning electron microscopic study of the vasculature of small intestine. Anat. Rec. 203:493-503.

44. Miller MM, Revel J-P. (1975). Scanning electron microscopy of epithelia prepared by blunt dissection. Anat. Rec. 183:339-358.

45. Moore SA, Bohlen HG, Miller BG, Evan AP. (1985) Cellular and vessel wall morphology of cerebral cortical arterioles after short-term diabetes in adult rats. Blood Vessels 22:265-277.

46. Mulvany MJ, Baandrup U, Gundersen HJG. (1985). Evidence for hyperplasia in mesenteric resistance vessels of spontaneously hypertensive rats using a three-dimensional dissector. Circ. Res. 57:794-800.

47. Mulvany MJ, Halpern W. (1977). Contractile properties of small arterial resistance vessels in spontaneously hypertensive and normotensive rats. Circ. Res. 41:19-26.

48. Murakami M, Sugita A, Shimada T, Nakamura K. (1979). Surface view of pericytes on the retinal capillary in rabbits revealed by scanning electron microscopy. Arch. Histol. Jpn 42:297-303.

49. Nagato T, Yoshida H, Yoshida A, Uehara Y. (1980). A scanning electron microscope study of myoepithelial cells in exocrine glands. Cell Tissue Res. 209:1-10.

50. Nordborg C, Johansson BB. (1979). The ratio between thickness of media and internal radius in cerebral, mesenteric and renal arterial vessels in spontaneously hypertensive rats. Clin. Sci. 57:27s-29s.

51. Ohashi Y, Kita S, Murakami T. (1976). Microcirculation of rat small intestine as studied by the injection replica scanning electron microscopic method. Arch. Histol. Japan 39:271-282.

52. Papa CM., Farber BF. (1971). Direct scanning electron microscopy of human skin. Arch. Derm. 104:262-270.

53. Rhodin JAG. (1980). Architecture of the vessel wall. In: Handbook of Physiology, Section 2, The Cardiovascular System II, Vol. 2, Vascular Smooth Muscle, DF Bohr, AP Somylo, HV Sparks, (eds.), Williams and Wilkins, Baltimore, MD, Ch. 1, p. 1.

54. Shimada T. (1981). Lymph and blood capillaries as studied by a new SEM technique. Biomedical Res. 2 Suppl. 243-248.

55. Shiraishi T, Sakaki S, Uehara Y. (1986). Architecture of the arterial vessels in the dog brain: A scanning electron-microscopic study. Cell Tissue Res. 243:329-335.

56. Short D. (1966). Morphology of the intestinal arterioles in chronic human hypertension. Brit. Heart J. 28:184-192.

57. Somylo AV. (1980). Ultrastructure of vascular smooth muscle. In: Handbook of Physiology, Section 2, The Cardiovascular System II, Vol. 2, Vascular Smooth Muscle, DF Bohr, AP Somylo, HV Sparks (eds.), Williams and Wilkins, Baltimore, MD, Ch. 2, p. 33.

58. Spencer PS, Lieberman AR. (1971). Scanning electron microscopy of isolated peripheral nerve fibers. Normal surface structure alterations proximal to neurons. Z. Zellorsch. 119:534-551.

59. Sterio DC. (1984). The unbiased estimation of number and sizes of arbitrary particles using the dissector. J. Microsc. 134:127-136.

60. Summerland BC, Greasey JM. (1975). A technique for preparing human dermal and scar specimens for scanning electron microscopy. J. Microsc. 103:369-376.

61. Uehara Y, Fujiwara T. (1984). The morphological changes of arterial smooth muscle cells upon vasodilation and vasoconstriction. In: Progress In Microcirculation Research II, FC Courtice, DG Garlick, MA Perry (eds.), Univ. of NSW, Sydney, Australia, pp. 405-410.

62. Uehara Y, Suyama K. (1978). Visualization of the adventitial aspect of the vascular smooth muscle cells under the scanning electron microscope. J. Electron Microsc.(Tokyo) 27:157-159.

63. Van Critters RL, Wagner BM, Rushmer RF. (1962). Architecture of small arteries during vasoconstriction. Circulation Res. 5:668-675.

64. Walmsley JG, Gore RW, Dacey RG, Damon DN, Duling BR. (1982). Quantitative morphology of arterioles from the hamster cheek pouch related to mechanical analysis. Microvas. Res. 24:249-271.

65. Weibel ER. (1979). Particle size and shape. In: Stereological Methods, Vol. 1, Academic Press, New York, NY, p. 162.

66. Weideman MP. (1968). Blood flow through terminal arterial vessels after denervation of the bat wing. Circ. Res. 22:83-89.

67. Whall CW, Myers MM, Halpern W. (1980). Norepinephrine sensitivity, tension development and neuronal uptake in resistance arteries from spontaneously hypertensive and normotensive rats. Blood Vessels 17:1-15.

68. Wolinsky H, Glasgov S. (1964). Structural basis for the static mechanical properties of the aortic media. Circ. Res. 14:400-413.

Discussion with Reviewers

RMKW Lee: It seems that for the same type of tissues (e.g. arterioles), there is no consistency that similar methods will work in the hands of different researchers. Even with the same researcher, results vary from one batch to another. Can you offer some possible explanation why this is happening?

Authors: There are several factors that can cause the results of the exposure technique to vary between researchers or batches. The principal factor that regulates reproducibility relates to how well each step of the procedure is controlled. In other words, the results of a particular experiment can be altered by simply changing just one condition of a single step in the overall protocol. The steps of the straight digestion procedures that need to be strictly controlled include the volume of tissue per volume of digesting media, temperature, duration of exposure, amount of agitation, method and degree of fixation, type of fixative(s), and source animal strictly controlled in order to reduce variations in results to a minimum. However, there is yet another significant factor that usually is not considered when attempting straight digestion methods- the amount of gross and/or microdissection. Most of the present methodologies designed to gain access to specific tissue(s) of interest by removing certain other tissue(s) incorporate activities that mechanically manipulate the target region. This manipulation alters the amount of tissue surrounding the tissue of and the permeability of the target region to the digestion media. The failure to recognize this latter factor will allow variations in the degree and quality of exposure that might appear to be inexplicable. In 1980, when we began to study ways to expose vessels for SEM, our initial failure to recognize this fact caused us to flounder during our effort to standardize the digestion protocol. In our opinion, the digestion step(s) are most effective at removing residual material loosely attached to the tissue of interest and basement membrane material associated with various tissues. We now feel we can anticipate the degree of exposure, based primarily on observations made during microdissection. We have also encountered clear variations in results due to investigating different types or strains of animals. Other factors include the type and amount of collagen surrounding a vessel. It is known that the condition is variable between species. Also, the structural organization of a tissue will include variations. An example is the degree of attachment the pial membrane has to the leptomeningial arteriolar bed. We have accommodated these variations through subtle adjustments during microdissection. Such variations may be addressed in future publications. In summary, close and careful monitoring of tissue handling is necessary in order to clarify and standardize one's best method for exposing the tissue(s) of interest.

RMKW Lee: Some methods for the removal of connective tissues do not include collagenase or elastase in the procedure. Is there any explanation why these methods work as well, if not better at times, than those which contain connective tissue enzymes?

Authors: Our experience has shown the connective tissue enzymes to be the most effective way to remove residual material loosely attached to the tissue of interest and basement membrane material. Fixation of the target region would alter the molecular structure and, therefore, the effectiveness of some connective tissue enzymes. The specificity of different types and batches of enzymes will alter their effectiveness. However, our experience with using chemical and/or enzyme media indicates that the effects of manipulation, as discussed above, has a major effect on a method's performance. This aspect usually is not taken into consideration when attempts are made to compare methodologies.

W Krizmanich: Do you think these various digestion methods cause cellular shrinkage?

Authors: Yes, we do. The precise cause of this shrinkage is not known. Other studies have suggested treating the specimen with uranyl acetate to reduce shrinkage during processing for SEM (Lee RMKW et. al. Scanning Electron Microsc.1979; III:439-448). Perhaps a similar treatment of tissues prior to digestion will reduce this phenomemon. Because of this problem, we make direct comparisons only between tissues treated identically (e.g., digested vs undigested). Only relative comparisons of results between tissues treated differently are appropriate.

A. Castenholz: We have some comments concerning the remarks and attempts of interpretation just in regard to our studies corresponding to numbers 11-13 of references cited in the manuscript. It seems to us that figure 2 alone is not suitable to characterize and assess our method of ultrasound treatment of vascular tissue to reveal structures of the outer vascular wall. This figure was only published to demonstrate the intramural positions of the "plastic strips" of a cast preparation, the "serendipitous" structures the paper no. 13 especially dealt with.

More informatory findings of SEM representation of vascular smooth muscle cells themselves and pericytic elements based on ultrasound treatment of small tissue slices were represented in the paper no. 12. We regret that the authors did not choose one or more figures (figures 1-4) of that contribution for their paper, which give clear evidence for the usability of the ultrasound treatment method although the question of its somewhat capricious reproducibility like other morphological methods should not be denied. Further applications of cast tissue preparations are given in another not cited paper: A. Castenholz, Scanning Electron Micros.1983; IV:1955-1962.

Authors: We chose not to include the additional reference (A. Castenholz, Scanning Electron Micros.1983; IV:1955-1962) suggested by the reviewer because we wished to focus this review on methods that will specificly expose the VSM. We recognize the potential of this methodology for examining the tissue elements surrounding the vasculature, but also recognize that all the other techniques also share this potential. We chose not to dwell on this potential at any point. Indeed, when focusing on the VSM, one could make an argument that the presence of such surrounding elements would be undesirable.